Available online at www.sciencedirect.com
ScienceDirect
Journal of Electroanalytical Chemistry 612 (2008) 37–41
Journal of Electroanalytical Chemistry
www.elsevier.com/locate/jelechem

# Electrochemical impedance sensing of DNA at PNA self assembled monolayer

Tesfaye Hailu Degefa, Juhyoun Kwak *

*Department of Chemistry, Korea Advanced Institute of Science and Technology (KAIST), Daejeon 305-701, Republic of Korea*

Received 29 May 2007; received in revised form 30 July 2007; accepted 5 September 2007
Available online 14 September 2007

**Abstract**

Monolayers of cysteine linked peptide nucleic acid (PNA) assembled on gold electrodes were investigated for the sensing of DNA recognition. The monolayer was characterized by cyclic voltammetry (CV). The electron transfer through the monolayers was investigated using electrochemical impedance spectroscopy (EIS) in the presence of target DNA and redox marker ions $[Fe(CN)_6]^{3-/4-}$ as hybridization indicator. The EIS spectra in the form of Nyquist plots were analyzed with a Randles circuit, and the electron transfer resistance, $R_{ct}$, was used to monitor the sensing of the target DNA. The results showed that without any modification to the target DNA, the complementary and the mismatch can be discriminated effectively at PNA self assembled monolayers (SAMs). Therefore, this work can provide another view on using PNA SAMs as a probe candidate for label-free detection of DNA recognition.


*Keywords:* Peptide nucleic acid; Self assembled monolayers; DNA; Label-free; Hybridization detection

## 1. Introduction

Over the last two decades, electrochemical DNA sensing approaches were mainly based on self assembled monolayers (SAMs) of DNA on electrode surfaces [1–3]. Recently, there has been an increasing interest for DNA sensors based on the SAMs of peptide nucleic acid (PNA) modified electrodes [4–6]. PNA is a DNA mimic that has a neutral peptide-like backbone with nucleobases that allows the molecule to hybridize to complementary DNA strands with high affinity and specificity [7]. DNA sensing at PNA surfaces based on quartz crystal microbalance [8], surface plasmon resonance [9,10], ion-sensitive filed effect transistor (IS-FET) [11,12] and electrochemistry [13–15] has been reported. Among the electrochemical sensors some involve PNA immobilized on an electrode surface as a probe for the recognition of the target DNA and a multiple charged electroactive species as hybridization indicator. The PNA assembled on the electrode surface as a probe is uncharged and does not affect the electron transfer from the negatively charged redox ions, such as $[Fe(CN)_6]^{3-/4-}$, to the electrode. Once the DNA target hybridizes to the surface immobilized PNA probe, there is a change in the interface and a change in the charge density at the SAMs of PNA. This change has been used as a means to develop a new class of sensors emerging as "ion-channel sensors" [16–19]. Electrochemical methods were used to monitor the influence of the charge on the current response of cyclic voltammetry (CV) for the electroactive marker ions $[Fe(CN)_6]^{3-/4-}$. The redox response of the marker ions changes with the hybridization of the target DNA to the PNA surface, because the extent of repulsion between the negatively charged marker ions and the phosphate background of the DNA depends on the degree of hybridization. Although observation of the current is simple for such system, electrochemical impedance spectroscopy (EIS) has been shown to provide prolific information about the barrier properties and sensitive to the interfacial electron transfer as revealed in the characterization of bimolecular-functionalized electrodes and biocatalytic

* Corresponding author. Tel.: +82 42 869 2833; fax: +82 42 869 2810.
*E-mail address:* Juhyoun_Kwak@kaist.ac.kr (J. Kwak).

0022-0728/$ - see front matter © 2007 Elsevier B.V. All rights reserved.
doi:10.1016/j.jelechem.2007.09.004

transformations at electrode surfaces [20–23]. It allows for the analysis of the interfacial changes originating from recognition events at the electrode surfaces.

Thus, in this paper we report EIS sensing of the target DNA at cysteine linked peptide nucleic acid (PNA) self assembled monolayers (SAMs) on gold electrode. The EIS spectra in the form of Nyquist plots were analyzed with a Randles circuit, and the charge-transfer resistance, $R_{ct}$, was used to monitor the sensing of the target DNA and the barrier properties of the PNA surfaces pended in the presence of the target DNA.

## 2. Experimental section

### 2.1. Chemicals and reagents

Unless otherwise indicated, all chemicals were obtained from Sigma or Aldrich and were used as received. The PNA probe conjugated with cysteine and all the target oligonucleotides employed in this work were synthesized and HPLC was purified by Panagene (Daejeon, Korea) and by GenoTech (Daejeon, Korea), respectively. The targets of hybridization were designed using perfect-matched (PM), single-base mismatched (SBM), and non-complementary (NC) oligonucleotides as shown in Table 1.

### 2.2. Electrochemical measurements

Cyclic voltammetry (CV) was performed using AUTOLAB 10 (Eco Chemie, Netherlands) interfaced with a personal computer. A standard three-electrode cell was used with either PNA SAMs modified or unmodified gold plate as a working electrode, $Hg|HgSO_4|K_2SO_4$ (sat) electrode (MSE) as a reference electrode and a Pt wire counter electrode. Using the frequency response analyzer (FRA) of AUTOLAB 10, the impedance spectra at a bias potential of −0.2 V (vs. MSE), which was superimposed on 5 mV rms sinusoidal potential modulations, were measured for 30 frequencies from 50 mHz to 2 kHz. The data are represented in the complex plane; Nyquist plots ($Z''$ vs. $Z'$, $Z''$ = imaginary impedance and $Z'$ = real impedance). The respective semicircle diameter corresponds to the charge-transfer resistance, $R_{ct}$, the values of which are calculated using the fitting program of AUTOLAB 10 (FRA, version 4.9 Eco Chemie, The Netherlands). The impedance spectra are fitted to a Randles equivalent electrical circuit for PNA modified electrode with/without the target DNA, including a solution resistance, $R_s$, a constant phase element (CPE), the charge-transfer resistance, $R_{ct}$, and a Warburg impedance, $Z_w$. From the regression, the charge-transfer resistance, $R_{ct}$, is obtained.

Chronocoulometric (CC) measurement was carried out with a pulse period of 500 ms and a pulse width of 600 mV (from +150 mV to −450 mV vs. Ag/AgCl). The electrode was allowed to equilibrate with $[Ru(NH_3)_6]^{3+}$ at +150 mV for 5 s before starting the potential step.

### 2.3. Electrode preparation

Gold electrodes were prepared by electron-beam evaporation of 40 nm of Ti followed by 150 nm of Au on Si (1 0 0) wafers. The electrode was cleaned in piranha solution (3:7 (v/v) 30% $H_2O_2$/ 70% $H_2SO_4$) for 4 min, followed by copious rinsing with distilled water and then dried with nitrogen gas. (*Warning: piranha reacts violently with organics*). The PNA SAMs modified electrode was constructed by immersing the clean gold substrate in a 20 μM PNA solution for *ca.* 20 h, rinsing with phosphate buffer (pH 7), then immersing in a 1 mM mercaptohexanol (MCH) solution for 1 h, and finally rinsing with the phosphate buffer and drying under a stream of nitrogen.

A surface coverage of $3.8 \times 10^{-12}$ mol/cm$^2$ PNA was estimated from the Cottrell's experiment with $[Ru(NH_3)_6]^{3+}$ and perfectly matched (PM) DNA target in a weak electrolyte [24,25]. The surface coverage of $[Ru(NH_3)_6]^{3+}$ was calculated as the difference in the chronocoulometic intercepts in the absence and presence of $[Ru(NH_3)_6]^{3+}$. The surface coverage of the $[Ru(NH_3)_6]^{3+}$ is then converted to DNA surface density with the relationship $\Gamma_{DNA} = \Gamma_0(z/m)$, where $\Gamma_{DNA}$ = the surface density of DNA, $\Gamma_0$ = the surface coverage of $[Ru(NH_3)_6]^{3+}$, $z$ = the charge of $[Ru(NH_3)_6]^{3+}$ and $m$ = the number of bases of DNA (see Fig. 1).

## 3. Results and discussion

The cysteine conjugated PNA self assembled monolayers (SAMs) on the gold surface were characterized by cyclic voltammetry (CV) using $[Fe(CN)_6]^{3-/4-}$ as electroactive marker ions. As shown in Fig. 2, a quasi-reversible redox cycle with increased peak-to-peak separation of 180 mV was observed. The unmodified gold surface shows a characteristic reversible redox cycle with peak-to-peak separation of 80 mV. This indicates that the SAMs of the PNA

Table 1
The sequence of oligonucleotide strands

| Name | Sequence |
|---|---|
| Cysteine conjugated PNA probe | Cys-O-CTG GCT TTG GTC CGT CT-$NH_2$ |
| Perfect matched DNA target (PM) | 5′-AGA CGG ACC AAA GCC AG-3′ |
| Single-base mismatched DNA target (SBM) | 5′-AGA CGG AC*A* AAA GCC AG-3′ |
| Non-complementary DNA target (NC) | 5′-GTC GAA GGT CTT ATA CA-3′ |

The Cys and O denote a cysteine group and ethylene glycol unit, respectively.

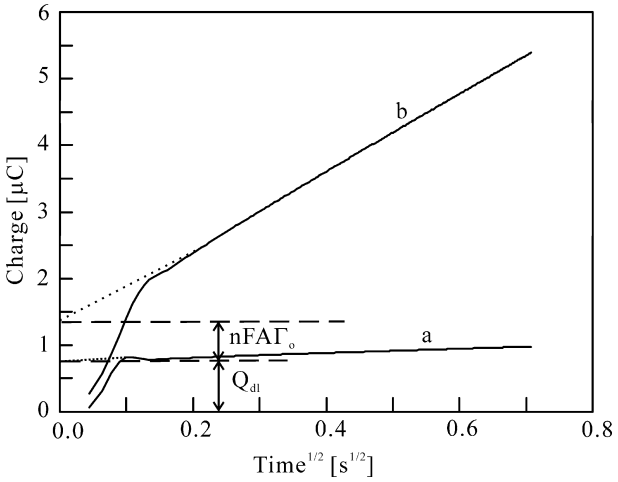


Fig. 1. Chronocoulometric response curve for the PNA-DNA modified Au electrode in 0 μM (a) and 50 μM (b). $[Ru(NH_3)_6]^{3+}$/10 mM Tris at pH 7.4. The dotted straight lines represent the extrapolated fits to the experimental data used to determine the intercept charges at $t = 0$.

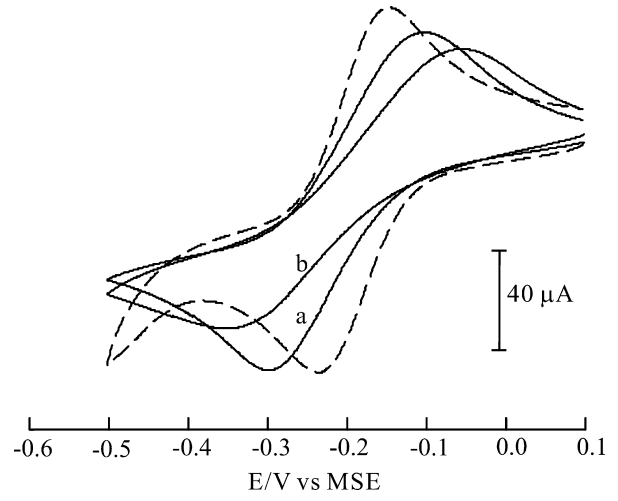


Fig. 2. CVs of 1 mM $[Fe(CN)_6]^{3-/4-}$ (1:1) in 20 mM phosphate buffer (pH 7) at scan rate of 50 mV/s for bare Au electrode (broken line) and for PNA modified Au electrode (solid line) (a) and (b) for PNA modified electrode incubated in target DNA (50 nM).

reduced the ability of the electron transfer between the solution and the underlying electrode. When the PNA modified electrode is incubated in a solution containing the target DNA, the peak-to-peak separation is further increased and the peak current is significantly decreased. However, the formal potential $(E^{0'} = (E_{pc} + E_{pa})/2)$ remains the same for both the PNA modified electrode and the PNA modified electrodes exposed to the target DNA.

As electrochemical impedance spectroscopy (EIS) provides more prolific information about the barrier properties [20–22], we have used EIS to describe the sensing of the target DNA at PNA surface and the barrier properties pended at the PNA modified electrode during the sensing of the target DNA. The EIS measurements were performed in the presence of $[Fe(CN)_6]^{3-/4-}$ as electroactive marker ions. Fig. 3-I shows the electrochemical impedance spectra (Nyquist plots, $Z''$ vs. $Z'$) for the PNA modified electrode exposed to the target DNA at different times. Each of the spectra is composed of a semicircle part in a high frequency region and a linear part in a low frequency region, corresponding to the electron transfer process and the diffusion process, respectively.

These spectra were modeled with the Randles equivalent circuit consisting of a solution resistance ($R_s$), charge-transfer resistance ($R_{ct}$), constant phase element (CPE), and Warburg impedance ($Z_w$) [26,27]. The diameter of the semicircle represents the charge-transfer resistance ($R_{ct}$) at the electrode surface. As shown in Fig. 3-I, the diameter of the semicircle, indicating the corresponding $R_{ct}$, increases as the hybridization time is increased. This change is attributed to the increase in the repulsive interaction (electrostatic and steric) between the redox marker ions and the electrode surface; the repulsion impedes the charge-transfer through the interface. The charge-transfer resistance, $R_{ct}$, increased faster during the first few minutes (~30 min) and then showed a gradual increment and

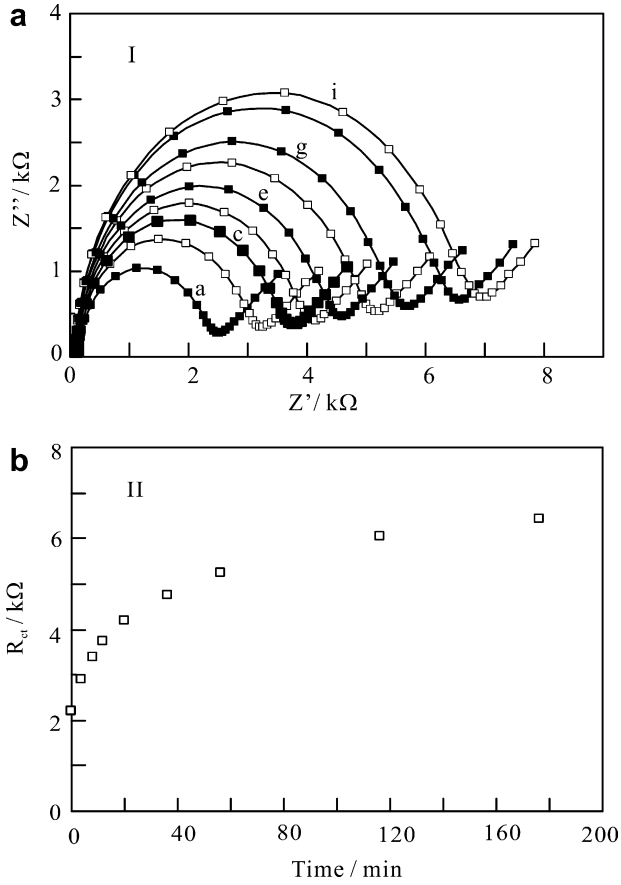


Fig. 3. (I) Impedance spectra at PNA modified Au electrode after sensing 200 nM target DNA in the presence of 1 mM $[Fe(CN)_6]^{3-/4-}$ (1:1) in 20 mM phosphate buffer (pH 7) for (a) 0, (b) 4, (c) 8, (d) 12, (e) 20, (f) 36, (g) 56, (h) 116 and (i) 176 min. (II) Plot of the dependance of the corresponding charge-transfer resistance, $R_{ct}$, with the hybridization time from plots in (I).

attained a plateau value after *ca*. 1 h, indicating that the hybridization reached its equilibrium (Fig. 3-II).

The sensing of DNA at the PNA SAMs was also investigated at different concentration of the target DNA. Fig. 4-I shows the response of the PNA surface for different concentration of target DNA. It was found that at lower target DNA concentration, a lower charge-transfer resistance, $R_{ct}$, was observed, and as the concentration was increased the resulting charge-transfer resistance, $R_{ct}$, was increased. This was observed directly from the diameter of the semicircle part of the spectra. This is the result of the negative charge of the DNA on the electrode surface decreasing the electron transfer of $[Fe(CN)_6]^{3-/4-}$ marker ion due to electrostatic repulsion. The charge-transfer resistance, $R_{ct}$, continued to increase until all possible recognition probes is accessed. As shown from the plot of $R_{ct}$ with the concentration of the target DNA, the charge-transfer resistance increased linearly and then does not show any significant increment with the increase of DNA (Fig. 4-II). It was also reported that the electrochemical behavior of fully complementary duplex would also increase the negative charge at the electrode surface, and would increase the charge-transfer resistance, $R_{ct}$, compared with the probe DNA alone [20].

The PNA surface was also studied for the sensing of mismatched target DNA. Fig. 5 shows the impedance spectra of the PNA modified electrodes after being exposed to different target DNA. The discrimination of the target DNA were investigated at three different concentrations, 50, 200 and 400 nM. These concentrations correspond to three different conditions on the plot of the charge-transfer resistance, $R_{ct}$, as a function of the concentration for the fully complementary target DNA (see Fig. 4-II).

The fully matched DNA resulted in a higher charge-transfer resistance, $R_{ct}$, than that of target mismatched DNA at higher target concentration. The non-complementary case has shown a much reduced effect at all target concentrations. As the EIS is used for the signal transduction at the uncharged PNA surface, the hybridization of the DNA leads to a signal, charge-transfer resistance $R_{ct}$, which is attributed to the amount of the DNA on the sensing surface. Thus, the relative surface coverage of the non-mismatched, i.e., perfectly matched (PM), and mismatched,

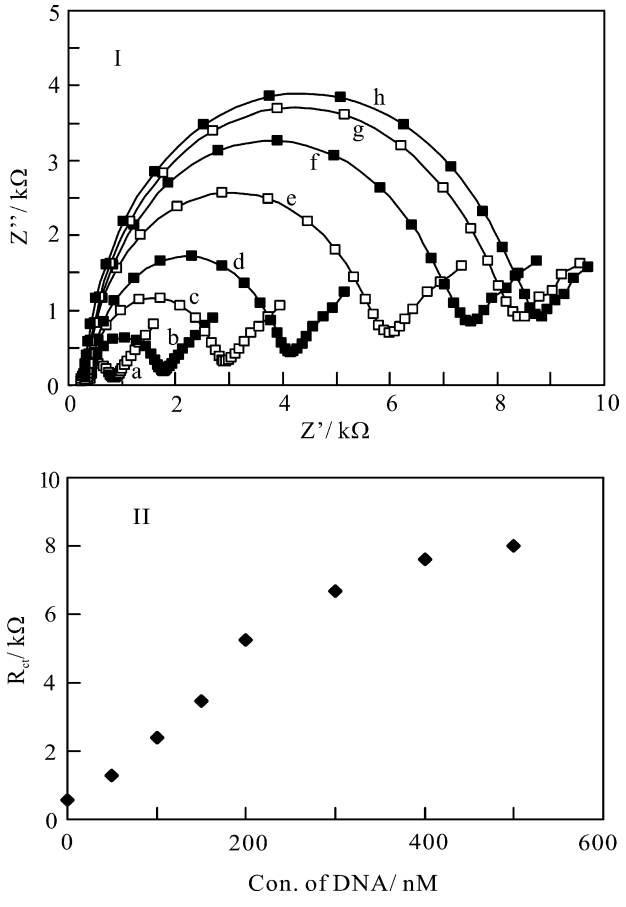


Fig. 4. (I) Impedance spectra at PNA modified Au electrode before (a) and after (b–h) addition of the target DNA: (a) 0, (b) 50, (c) 100, (d) 150, (e) 200, (f) 300, (g) 400, and (h) 500 nM in the presence of 1 mM $[Fe(CN)_6]^{3-/4-}$ (1:1) marker ions in 20 mM phosphate buffer (pH 7). The hybridization time is 20 min. (II) Plot of the dependance of the corresponding electron transfer resistance, $R_{ct}$, with concentration of the target DNA.

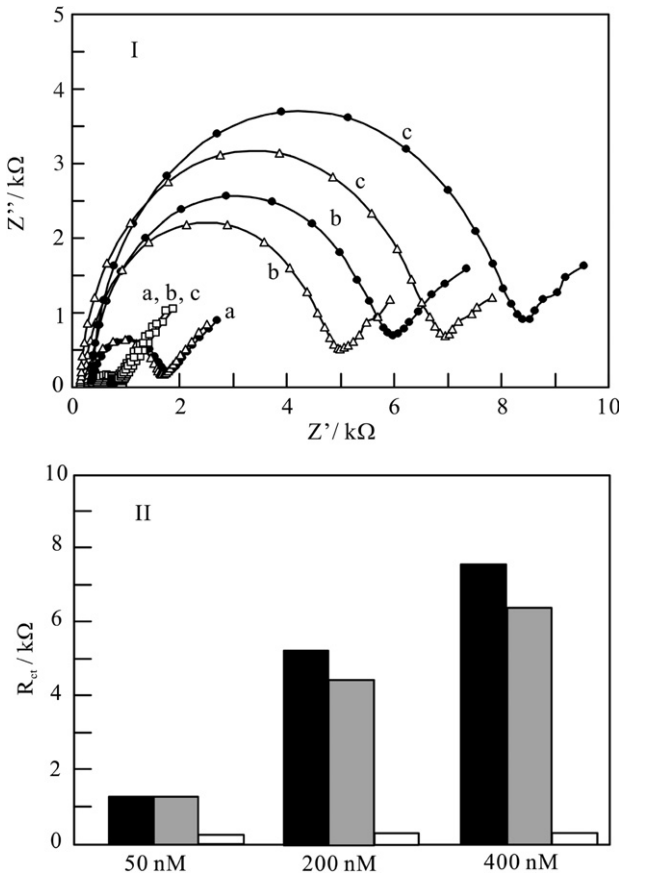


Fig. 5. (I) Impedance spectra at PNA modified Au electrode in the presence of 1 mM $[Fe(CN)_6]^{3-/4-}$ (1:1) marker ions in 20 mM phosphate buffer (pH 7) with 50 (a), 200 (b) and 400 nM (c) of PM (filled circle), SBM (triangle) and NC (square). (II) Plot of the corresponding charge-transfer resistance, $R_{ct}$, with concentration of the target DNA; 50, 200 and 400 nM of PM (black), SBM (gray) and NC (white).

i.e., single-base mismatched (SBM) and non-complementary (NC), DNA targets can be estimated from the relative values of the charge-transfer resistances, $R_{ct}$. The values are 1.2 for PM vs. SBM and 23.9 for PM vs. NC at 400 nM target DNA concentration (Fig. 5).

## 4. Conclusion

In this study, we have demonstrated the EIS sensing of DNA at PNA SAMs modified electrode surface. Without any modification to the target, the complementary and the mismatch can be discriminated effectively. Finally this method could further improved through the re-designing of the PNA surfaces and through further steps for the signal amplification. Therefore, the principle of impedimetric sensing of DNA using PNA as a probe is a promising potential candidate for label-free detection of DNA recognitions.

## Acknowledgement

This work was supported by the Korea Science and Engineering Foundation (KOSEF) Grant funded by the Korean Government (MOST) through the Bioelectronics Program (M10536000001-06N3600-00110), the Basic Research Program (R01-2005-000-10503-0), and the National R&D Project for Nano Science and Technology.

## References

[1] P. de-los-Santos-Alvarez, M.J. Lobo-Castanon, A.J. Miranda-Ordieres, P. Tunon-Blanco, Anal. Bioanal. Chem. 378 (2004) 104.
[2] K. Kerman, M. Kobayashi, E. Tamiya, Meas. Sci. Technol. 15 (2004) R1.
[3] T.G. Drummond, M.G. Hill, J.K. Barton, Nature Biotechnol. 21 (2003) 1192.
[4] J. Wang, Biosensors Bioelectron. 13 (1998) 757.
[5] C. Briones, E. Mateo-Marti, C. Gomez-Navarro, V. Parro, E. Roman, J.A. Martin-Gago, Phys. Rev. Lett. 20 (2004) 208103.
[6] S. Shakeel, S. Karim, A. Ali, J. Chem. Technol. Biotechnol. 81 (2006) 892.
[7] P.E. Nielsen, M. Egholm, R.H. Berg, O. Buchardt, Science 254 (1991) 1497.
[8] J. Wang, P.E. Nielsen, M. Jiang, X. Cai, J.R. Fernandes, D.H. Grant, M. Ozsoz, A. Beglieter, M. Mowat, Anal. Chem. 69 (1997) 5200.
[9] T. Endo, K. Kerman, N. Nagatani, Y. Takamura, E. Tamiya, Anal. Chem. 77 (2005) 6976.
[10] J. Liu, L. Tiefenauer, S. Tian, P.E. Nielsen, W. Knoll, Anal. Chem. 78 (2006) 470.
[11] T. Uno, H. Tabata, T. Kawi, Anal. Chem. 78 (2007) 52.
[12] T. Ohtake, Electrochemistry 74 (2006) 114.
[13] K. Kerman, D. Ozkan, P. Kara, A. Erdem, B. Meric, P.E. Nielsen, M. Ozsoz, Electroanalysis 15 (2003) 667.
[14] K. Kerman, M. Vestergaard, N. Nagatani, Y. Takamura, E. Tamiya, Anal. Chem. 78 (2006) 2182.
[15] H. Aoki, P. Buhlmann, Y. Umezawa, Electroanalysis 12 (2000) 1272.
[16] E. Bakker, Y. Qin, Anal. Chem. 78 (2006) 3965.
[17] P. Schon, T.H. Degefa, A. Asaftei, W. Meyer, L. Walder, J. Am. Chem. Soc. 127 (2005) 11486.
[18] Y. Umezawa, H. Aoki, Anal. Chem. 76 (2004) 320a.
[19] H. Aoki, Y. Umezawa, Analyst 128 (2003) 681.
[20] A. Bardea, F. Patolsky, A. Dagan, I. Willner, Chem. Commun. (1999) 21.
[21] L. Alfonta, A. Bardea, O. Khersonsky, E. Katz, I. Willner, Biosensors Bioelectron. 16 (2001) 675.
[22] F. Patolsky, A. Lichtenstein, I. Willner, J. Am. Chem. Soc. 123 (2001) 5194.
[23] B. Pejcic, R.D. Marco, Electrochem. Acta 51 (2006) 6217.
[24] A.M. Steel, T.M. Herne, M.J. Tarlov, Anal. Chem. 70 (1998) 4670.
[25] E.L.S. Wong, J.J. Gooding, J. Am. Chem. Soc. 129 (2007) 8950.
[26] S.M. Park, J.S. Yoo, Anal. Chem. 75 (2003) 455a.
[27] A.J. Bard, L.R. Faulkner, Electrochemical Methods; Fundamentals and Applications, Wiley, New York, 2001.